Dynamics of ANS Binding to Tuna Apomyoglobin Measured with Fluorescence Correlation Spectroscopy

Ettore Bismuto,* Enrico Gratton,† and Don C. Lamb†

*Departimento di Biochimica e Biofisica, Seconda Universita di Napoli, 80138 Napoli, Italy; and †Department of Physics, University of Illinois at Urbana-Champaign, Urbana, Illinois 61801-3080 USA

ABSTRACT The dynamics of the binding reaction of ANS to native and partly folded (molten globule) tuna and horse apomyoglobins has been investigated by fluorescence correlation spectroscopy and frequency domain fluorometry. The reaction rate has been measured as a function of apomyoglobin and ANS concentrations, pH, and temperature. Examination of the autocorrelation functions shows that the reaction rate is fast enough to be observed in tuna apomyoglobin, whereas the reaction rate in horse apomyoglobin is on the same time scale as diffusion through the volume or longer. Specifically, for tuna apomyoglobin at pH 7 and room temperature the on rate is 2200 $\mu M^{-1}\ s^{-1}$ and the off rate is 5900 s^{-1}, in comparison with $k_{on} = 640\ \mu M^{-1}\ s^{-1}$ and $k_{off} = 560\ s^{-1}$ for horse myoglobin as measured previously. The independence of the reaction rate from the ANS concentration indicates that the reaction rate is dominated by the off rate. The temperature dependence of the on-rate shows that this rate is diffusion limited. The temperature dependence of the off rates analyzed by Arrhenius and Ferry models indicates that the off rate depends on the dynamics of the protein. The differences between horse and tuna apomyoglobins in the ANS binding rate can be explained in terms of the three-dimensional apoprotein structures obtained by energy minimization after heme removal starting from crystallographic coordinates. The comparison of the calculated apomyoglobin surfaces shows a 15% smaller cavity for tuna apomyoglobin. Furthermore, a negative charge (D44) is present in the heme cavity of tuna apomyoglobin that could decrease the strength of ANS binding. At pH 5 the fluorescence lifetime distribution of ANS-apomyoglobin is bimodal, suggesting the presence of an additional binding site in the protein. The binding rates determined by FCS under these conditions show that the protein is either in the open configuration or is more flexible, making it much easier to bind. At pH 3, the protein is in a partially denatured state with multiple potential binding sites for ANS molecule, and the interpretation of the autocorrelation function is not possible by simple models. This conclusion is consistent with the broad distribution of ANS fluorescence lifetimes observed in frequency domain measurements.

INTRODUCTION

Proteins are systems capable of displaying a large set of conformational fluctuations even at thermodynamic equilibrium because of their marginal stability (Jaenicke and Lilie, 2000). These fluctuations range in timescale from picoseconds to seconds (Cooper and Hoube, 1988). A detailed understanding of proteins and how they function require knowledge of protein dynamics in all of the various timescales. Spectroscopic methods such as frequency domain fluorometry (Gratton and Limkeman, 1983) are very efficient for investigating protein dynamics in the nanosecond time scale. Stopped-flow techniques detected by circular dichroism or by steady-state fluorescence properties are extensively used to explore in proteins dynamic processes longer than millisecond time scale needed for effectively mixing the solutions (Hiromi, 1979). Many fundamental events occurring in the protein folding as well as important catalytic steps are faster than milliseconds (Clarke et al., 1999; Holtzer et al., 2001; Farazi et al., 2000). Relaxation experiments such as flash photolysis and temperature jump experiments are excellent for measuring dynamics on the microsecond timescale if the dynamics of interest can be synchronized. Unfortunately, many dynamic processes in proteins occurring on the microseconds to milliseconds time scales cannot be synchronized and are more difficult to measure. Phosphorescence techniques can be usefully employed but have no general applicability (Broos et al., 2001; Cioni and Strambini, 1998).

FCS is an emerging fluorescence technique in which temporal fluctuations in the fluorescence intensity from a sample of fluorescent molecules are analyzed to obtain information about the processes that give rise to the fluorescence fluctuations (Thomson, 1991; Lamb et al., 2000). The fluctuations may arise from several sources such as variation in the number of fluorescent molecules within the observation volume due to translational diffusion (Magde et al., 1974), rotational diffusion (Ehrenberg and Rigler, 1974; Aragón and Pecora, 1976; Kask et al., 1989), triplet-state excitation (Widengren et al., 1994; Widengren et al., 1995), conformational motions (Bonnet et al., 1998; Haupts et al., 1998), and chemical reactions (Magde et al., 1972, 1974; Magde, 1976; Rauer et al., 1996; Lamb et al., 2000). For FCS measurements in an open volume, the measured fluctuations must occur in the time that the molecule diffuses through the observation volume. In this article, we demon-

Received for publication 11 May 2001 and in final form 8 August 2001.

The authors are listed in alphabetical order.

Address reprint requests to Dr. Ettore Bismuto, Dipartimento di Biochimica e Biofisica, Seconda Università di Napoli, Via Costantinopoli, 16 80138 Napoli, Italy. Tel.: 39-081-566-7635; fax: 39-081-566-5863; E-mail: ettore.bismuto@unina2.it.

Abbreviations: ANS, 1-anilino-8-naphthalene sulfonic acid; FCS, fluorescence correlation spectroscopy; ACF, autocorrelation function; APD, avalanche photodiode.

0006-3495/01/12/3510/12 $2.00

strate how FCS can be a very powerful technique to explore protein dynamics in the microsecond time region. Because FCS is an equilibrium technique, no perturbation of the sample is necessary to synchronize the dynamics of the protein. In addition, FCS can be performed at very low protein concentrations minimizing protein aggregation and making FCS well suited for investigating protein denaturation and refolding.

The fluorophore we use for our FCS experiments is ANS, a charged hydrophobic fluorescent molecule, which has been extensively used as an extrinsic probe of protein macromolecules. ANS is strongly fluorescent when bound to the protein and essentially nonfluorescent when surrounded by water. The large use of this fluorophore is due to the dramatic enhancement of its fluorescence and the shift of the emission maximum to shorter wavelengths when surrounded by nonpolar amino acid residues of proteins. After the original experiments of Stryer on sperm whale apomyoglobin that binds ANS in the heme pocket (Stryer, 1965), a large number of studies have been reported in the last three decades concerning other native proteins able to bind ANS to obtain structural characterizations of specific protein environments. More recent investigations observed the ability of ANS molecules to bind to nonnative structural states of proteins with a pronounced secondary structure and compactness but without a tightly packed tertiary structure, e.g., "molten globule" state. This study prompted a series of articles concerning the interactions of ANS with partially unfolded states of proteins. Currently, ANS represents a standard probe for investigating the population of compact partially folded intermediate states of proteins (Demarest et al., 2001; Li and Jing, 2000; Khan et al., 2000; Bedell et al., 2000; Bhattacharyya et al., 2000; Zhou et al., 2000; Ali et al., 1999; Muzammil et al.1999). Furthermore, some articles have been recently published concerning aggregation of nonnative protein molecules such as the infectious scrapie agents in which the characteristics of metastable forms are monitored by ANS fluorescence spectroscopy (Kundu and Guptasarma, 1999; Safar et al., 1994). Here we present the results of the bimolecular reaction of ANS and apomyoglobin both in the native state as well as at acidic pH where apomyoglobin occurs in a molten globule state that has served as a paradigm for understanding the role of partially folded states in protein folding (Hughson et al., 1990; Bismuto and Irace, 1994). Our results demonstrate the ability of FCS to determine the microscopic rate coefficients of bimolecular reactions and the possibility to use ANS to measure the protein dynamics of apomyoglobin at different temperatures and pH values in time windows ranging from microseconds to milliseconds.

Autocorrelation function analysis

An FCS measurement results in a time series of photon arrival times that can be analyzed directly in hardware or later with software using various techniques. An autocorrelation analysis provides information over the correlation time of the intensity fluctuations present in the data and hence information about the dynamics of the system. For two-photon excitation such as that used in this work, the fluorescence intensity of a single fluorescent species is given by:

$$F(t) = \frac{1}{2}\kappa\sigma Q\int d\mathbf{r}C(\mathbf{r}, t)W(\mathbf{r}), \tag{1}$$

in which κ is the detection efficiency, σ is the two-photon absorption cross-section at the wavelength of excitation, Q is the fluorescence quantum yield, $C(\mathbf{r}, t)$ is the number density, and $W(\mathbf{r})$ is a function that describes the observation volume that is the overlap between the square of the point spread function of the laser, the extent of the sample, and the detection volume. The normalized ACF is defined as:

$$G(\tau) = \frac{\langle F(t)F(t+\tau)\rangle - \langle F(t)\rangle^2}{\langle F(t)\rangle^2}, \tag{2}$$

in which $\langle\ \rangle$ denotes the time average. The time and ensemble averaged values are independent of the measurement time t if the sample is stationary and does not significantly photobleach during the measurement.

At dilute concentrations of freely diffusing particles in an open volume, the thermodynamic fluctuations in the number of molecules within the observation volume is detectable in the fluorescence intensity. The ACF for a single, freely diffusing fluorescent species in an open volume can be determined analytically provided $W(\mathbf{r})$ can be approximated by a three-dimensional Gaussian. For a three-dimensional Gaussian observation volume with radial dimension w_r (the distance to $1/e^2$ in intensity) and axial dimension w_z, the ACF is given by:

$$G_{\text{Diff}}(\tau, N, D) = \frac{\gamma}{\langle N\rangle}\left(\frac{1}{1+8D\tau/w_r^2}\right)\left(\frac{1}{1+8D\tau/w_z^2}\right)^{1/2} \tag{3}$$

in which $\gamma = (1/2)^{3/2}$ is a geometrical factor, $\langle N\rangle$ is the average number of molecules in the excitation volume, and D is the diffusion coefficient of the molecule.

Bimolecular reaction

Changes in the fluorescence intensity due to chemical reactions are also observable in the ACF if the fluctuations occur during the transit time of the molecule through the observation volume. An analytical expression can be derived for a bimolecular reaction between a macromolecule, M, and a ligand, L:

$$M + L \underset{k_{\text{off}}}{\overset{k_{\text{on}}}{\rightleftharpoons}} ML, \tag{4}$$

provided the ligand is small enough that the diffusion of the macromolecule is unaffected when the ligand is bound (i.e., $D_M = D_{ML} = D$) and the reaction rate, k_r, occurs much faster than the diffusion of the ligand through the observation volume, i.e., $k_r \gg D_1/w_r^2$. The reaction rate is given by:

$$k_r = k_{on}(\langle C_L\rangle + \langle C_M\rangle) + k_{off}, \quad (5)$$

and the ACF is given by:

$$\begin{aligned} G(\tau) = {} & G_{Diff}(\tau,N_M + N_{ML},D_M)(\mathcal{T}_M + \mathcal{T}_{ML})^2 \\ & + \frac{G_{Diff}(\tau,1,D^+)}{k_r}\left[\frac{\langle C_{ML}\rangle}{\langle C_M\rangle}\frac{k_{on}\langle C_M\rangle}{\langle N_M + N_{ML}\rangle}\right. \\ & \times\left(\mathcal{T}_M - \mathcal{T}_{ML}\frac{\langle C_M\rangle}{\langle C_{ML}\rangle}\right)^2 - \frac{k_{on}\langle C_M\rangle}{\langle N_M\rangle}\mathcal{T}_L \\ & \left.\times\left(\mathcal{T}_M - \mathcal{T}_{ML}\frac{\langle C_M\rangle}{\langle C_{ML}\rangle}\right) + \frac{(k_{on}\langle C_L\rangle + k_{off})}{\langle N_L\rangle}(\mathcal{T}_L)^2\right] \\ & + \frac{G_{Diff}(\tau,1,D^-)}{k_r}\left[\frac{\langle C_{ML}\rangle(k_{on}\langle C_L\rangle + k_{off})}{\langle C_M\rangle\ \langle N_M + N_{ML}\rangle}\right. \\ & \times\left(\mathcal{T}_M - \mathcal{T}_{ML}\frac{\langle C_M\rangle}{\langle C_{ML}\rangle}\right)^2 + \frac{k_{on}\langle C_M\rangle}{\langle N_M\rangle}\mathcal{T}_L \\ & \left.\times\left(\mathcal{T}_M - \mathcal{T}_{ML}\frac{\langle C_M\rangle}{\langle C_{ML}\rangle}\right) + \frac{k_{on}\langle C_M\rangle}{\langle N_L\rangle}(\mathcal{T}_L)^2\right]e^{-k_r\tau} \quad (6) \end{aligned}$$

in which $\mathcal{T}_i$ refers to the fractional intensity of the i^{th} species,

$$D^+ = \left[D_L\frac{\langle C_L\rangle}{\langle C_L\rangle + \langle C_{ML}\rangle f} + D_M\frac{\langle C_{ML}\rangle f}{\langle C_L\rangle + \langle C_{ML}\rangle f}\right],$$

$$D^- = \left[D_L\frac{\langle C_{ML}\rangle f}{\langle C_L\rangle + \langle C_{ML}\rangle f} + D_M\frac{\langle C_L\rangle}{\langle C_L\rangle + \langle C_{ML}\rangle f}\right],$$

and

$$f = \frac{\langle C_M\rangle}{\langle C_M\rangle + \langle C_{ML}\rangle}$$

This formula can be significantly simplified when working with an excess of ligand. However, because ANS is weakly fluorescent in water, we have worked at lower ANS concentrations to minimize background fluorescence. To determine the on and off rate constants directly from Eq. 6, it is necessary to know the relative intensities of the various reactants. The fractional intensities can also be written in terms of either the absolute or relative molecular brightness, ϵ,

$$\mathcal{T}_i = \frac{\varepsilon_i\langle C_i\rangle}{\varepsilon_M\langle C_M\rangle + \varepsilon_{ML}\langle C_{ML}\rangle + \varepsilon_L\langle C_L\rangle}. \quad (7)$$

For a more complete treatment of the determination of the ACF for reactions, we refer the reader to Lamb et al. (2000), Thomson (1991), and Elson and Madge (1974).

MATERIAL AND METHODS

ANS binding to apomyoglobin

ANS is a naphthalene dye that is strongly quenched by water and undergoes a dramatic increase in fluorescence intensity when it binds to hydrophobic regions of proteins. ANS binds to apomyoglobin in the cavity where the heme group would normally reside with a stoichiometry of 1:1 at pH 7. In buffer, the fluorescent quantum yield of ANS is less than 0.004, the fluorescent lifetime is less than 85 ps (Bismuto et al. 1996), and the emission maximum is at 515 nm. Upon binding to the hydrophobic heme pocket of myoglobin, the fluorescent intensity of the ANS increases by ~200 fold, the fluorescent quantum efficiency becomes ~1, the fluorescence lifetime increase to 12 to 16 ns, and the fluorescence emission maximal shifts to 465 nm.

Sample preparation

All common reagents were purchased from Sigma (St. Louis, MO). ANS was from Molecular Probes (Eugene, OR) and was tested by an high-performance liquid chromatography reverse-phase procedure. The ANS concentration was determined spectrophotometrically using 4.95×10^3 cm^{-1} M^{-1} as the molar absorption coefficient at 350 nm (Weber and Young, 1964).

Horse myoglobin was purchased from Sigma; the protein was used after purification by fast liquid chromatography using a superdex-75 column (10 mm × 25 cm) from Pharmacia (Piscataway, NJ) equilibrated with 50 mM sodium phosphate buffer at pH 7.0. The main component of tuna myoglobin was extracted from heart ventricle muscle and purified according to the method described by Bismuto et al. (1989). The protein homogeneity was controlled by sodium dodecyl sulfate polyacrylamide gel electrophoresis with 15% gel and 5% stacking gel. The myoglobin concentrations were determined spectrophotometrically in the Soret region using molar absorption coefficients of 157,000 and 137,000 cm^{-1} M^{-1} for horse and tuna myoglobin respectively (Bismuto et al., 1985).

The heme was removed from myoglobin by 2-butanone extraction procedure (Teale, 1959). The heme contamination of apoprotein was assessed spectrophotometrically. In all cases, no significant absorption was observed in the Soret region. The concentration of apomyoglobin was determined by absorption at 280 nm. The absorption molar coefficients were calculated from tryptophan and tyrosine content (Wetlaufer, 1962). The resulting values were 13,500 and 8500 cm^{-1} M^{-1} for horse and tuna apomyoglobin, respectively.

FCS setup

The two-photon excitation FCS setup consists of an Argon-Ion pumped Ti:Sapphire laser (Coherent, Mira 900), an epi-illuminated fluorescence microscope (Zeiss, Axiovert 135 TV), and an APD (EG&G, SPCM-AQ-161). The Ti:Sapphire laser was run at 76 MHz with a pulse width of 150 fs at a wavelength of 787 ± 11 nm (full width at half maximum). The laser was focused into the sample by a 63 × oil-immersion 1.4 numerical aperture objective (Zeiss, Plan-Apochromat). The resulting fluorescence was collected through the same objective and separated from the laser light by a dichroic mirror (Chroma, 640DCSPXR) and filter (Schott, BG39). The fluorescence was focused onto an APD that was operated in single-photon counting mode. The output of the APD was recorded using a home-built photon counting card that has been commercialized by Industria Strumentazioni Scientifiche (F201CB) at a frequency of 10 MHz. The calculation and fitting of the ACF was performed after data collection in software with programs written using PVWave (version 6.21, Visual Numerics, Inc). One advantage of storing the entire time series of photon arrival to disk is that we were able to remove intensity spikes in the fluorescence due to impurities or aggregation from the data series and

analyze the remainder of the record. The calculated ACF was corrected for afterpulsing, as discussed in the Appendix.

Fluorescence emission decay of ANS-apomyoglobin complex

Frequency domain techniques were used to measure the fluorescence decay of all samples in the range between 1 and 200 MHz (Gratton and Limkeman 1983). The light source was a high repetition mode-locked Nd:YAG laser. This laser is used to synchronously pump a dye laser, whose pulse train is frequency doubled with an angle-tuned frequency doubler (Alcalà et al., 1985). The excitation wavelength was 350 nm, and the beam was polarized at the "magic angle" to eliminate rotational effects from the fluorescence lifetime measurements. The fluorescence emission was observed through a long-wave pass filter with a cutoff wavelength at 400 nm (Corion LG-400-F). A solution of *p*-bis-(2-(5-phenyloxozonolyl)) benzene in ethanol served as the lifetime reference. The temperature was monitored continuously during measurements by attaching a thermocouple to the sample cuvette. The output of the thermocouple was displayed by an Omega Digicator (from Omega Engineering) with an accuracy of ±0.1°C. The data were analyzed using Global Unlimited as described previously (Beechem, 1992). The quality of the fit was assessed from the reduced chi square values and the plots of weighted residuals.

Computer simulation

The 1MYT and 1YMB protein databank files of tuna and horse metmyoglobins (Birnbaum et al., 1994; Evans and Brayer, 1990) were used to extract starting sets of apomyoglobin coordinates for energy minimization using the GROMOS96 software package (Van Gunsteren et al., 1996). Three cycles of 50,000 steps of minimization by steepest descent and conjugate gradients were performed using GROMOS 43B1 force field in vacuo without a reaction field. Molecular surface cavity and electrostatic potentials were calculated using coulombic potential and only charged residues. The solvent and protein dielectric constant values used in the calculation were 80 and 4.0, respectively. Molecular surface, electrostatic potential, heme cavity residues, as well as minimized apomyoglobin structures were visualized by Swisse-Pdb-Viewer v3.7b2 (Guex and Peitsch, 1997).

RESULTS

Verification of the ANS binding reaction in the autocorrelation function

The observation volume was calibrated with a solution of 2 nM tetramethylrhodamine using the known diffusion coefficient of 280 $\mu m^2/s$ (Rigler et al., 1993). Characteristic ACFs for FCS measurements of mixtures of 500 nM ANS with either 1 μM tuna apomyoglobin or 1 μM horse apomyoglobin at pH 7 are shown in Fig. 1. To determine if the observed correlation was due to the binding of ANS to apomyoglobin, the ACF was fit to the expression for diffusion alone (Eq. 3) and to the ACF for a bimolecular reaction of freely diffusion particles through an open volume where the reaction rate is much faster than the rate of diffusion through the observation volume (Eq. 6). Fitting the measured autocorrelation to the ACF for diffusion alone yielded diffusion coefficients of $D_{Tuna} = 360\ \mu m^2/s$, and $D_{Horse} = 90\ \mu m^2/s$. The diffusion coefficient for horse myoglobin is

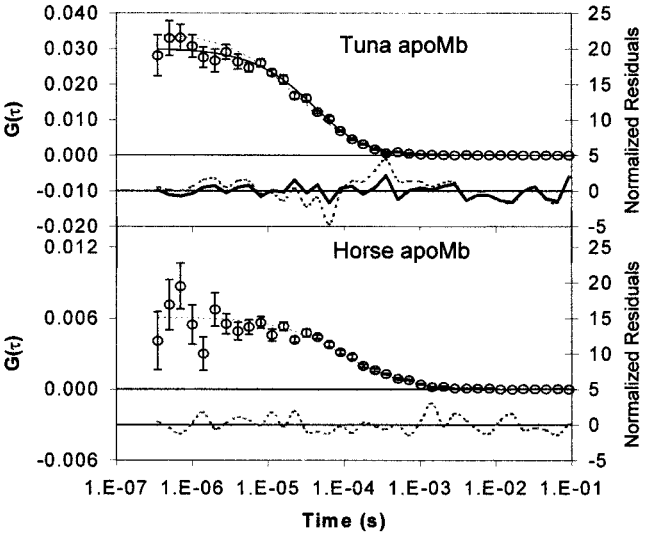

FIGURE 1 The ACF of ANS and tuna apomyoglobin (*top*) and ANS and horse apomyoglobin (*bottom*) at pH 7.0 with the normalized residuals. The dashed lines (*top* and *bottom*) are fits of the respective ACFs to diffusion alone (Eq. 3) and the solid line (*top*) is a fit to a bimolecular reaction (Eq. 6).

consistent with the values measured using labeled myoglobins (D. C. Lamb, unpublished results), whereas the diffusion rate for tuna is faster than that of tetramethylrhodamine and clearly cannot be the diffusion of the protein. As can be seen in the residuals, there is an improvement in the fit to the ACF of tuna myoglobin ANS when using the bimolecular reaction model. Both results suggest that the reaction rate is fast enough to be observed in tuna apomyoglobin, whereas the reaction rate in horse is on the same time scale as diffusion through the volume or longer.

To verify that the observed correlation is due to the reaction of ANS with apomyoglobin and not due to light induced fluctuations or diffusion of impurities within the sample, a second FCS measurement was made with a different laser power and observation volume. The change in observation volume was performed by replacing the 63× plan-Apochromat oil-immersion objective with a 40× Fluar oil immersion objective (numerical aperture = 1.3). The 40× objective has a larger back aperture than the 63× objective and was under filled for this measurement. The decay time of the ACF of ANS and tuna apomyoglobin was independent of the observation volume and laser intensity, ruling out the possibility that the observed fluctuations in fluorescence intensity are either photo induced or come from impurities in the sample. For ANS and horse apomyoglobin, the decay time of the ACF increased with increasing volume, suggesting that the observed fluctuations are coming from diffusion of the ANS apomyoglobin complex through the observation volume and that the reaction rate is on the same timescale as diffusion through the volume or longer. The slower reaction of ANS binding to horse apo-

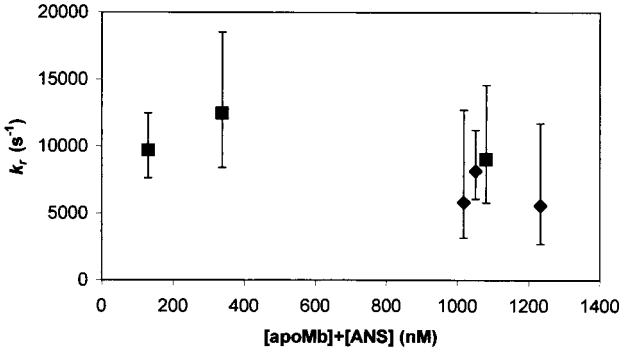

FIGURE 2 The reaction rate of ANS binding to tuna apomyoglobin as a function of the total of the ANS and protein concentrations. ♦, Measurements made at constant (50 nM ANS) concentration; ■, measurements made at constant (1000 nM) protein concentration.

myoglobin is consistent with the results reported by Lamb et al. (2000).

Determination of on and off rates

From the fit of the ACF, we can directly extract the on and off rate constants. For tuna apomyoglobin at pH 7 and room temperature, $k_{on} = 2200\ \mu M^{-1}\ s^{-1}$ and $k_{off} = 5900\ s^{-1}$. The reaction rate of ANS binding to apomyoglobin has been measured as a function of apomyoglobin and ANS concentrations, pH, and temperature. A plot of the reaction rate versus total apomyoglobin and ANS concentrations is shown in Fig. 2. The reaction rate appears to be independent of concentration, suggesting that the reaction rate is dominated by k_{off}. Fig. 3 shows k_{on} and k_{off} as a function of temperature and pH. The on rate constant was fit with a simple diffusion-limited reaction model, whereas the off rate constant was fit with an Arrhenius and a Ferry temperature dependence. The fit parameters are given in Table 1.

Fluorescence lifetime distribution

The fluorescence emission decay of the tuna ANS-apoMb complex was investigated as function of pH. The data were analyzed either as a sum of discrete exponentials or using continuous-lifetime distribution models: the best fits were obtained using Lorentzian distributions of lifetimes.

The resulting lifetime distributions are shown in Fig. 4, and the corresponding fit parameters relative to neutral pH, pH 4.9, and pH 3.0 are summarized in Table 2. The main emission component displays a lifetime value ranging from 13 to 16 ns with the shorter peak lifetimes corresponding to more acidic conditions. These values are consistent with the hydrophobic characteristics of the ANS binding region in apomyoglobin. The decrease in the center value can result from an increase in solvent accessibility, changes in the

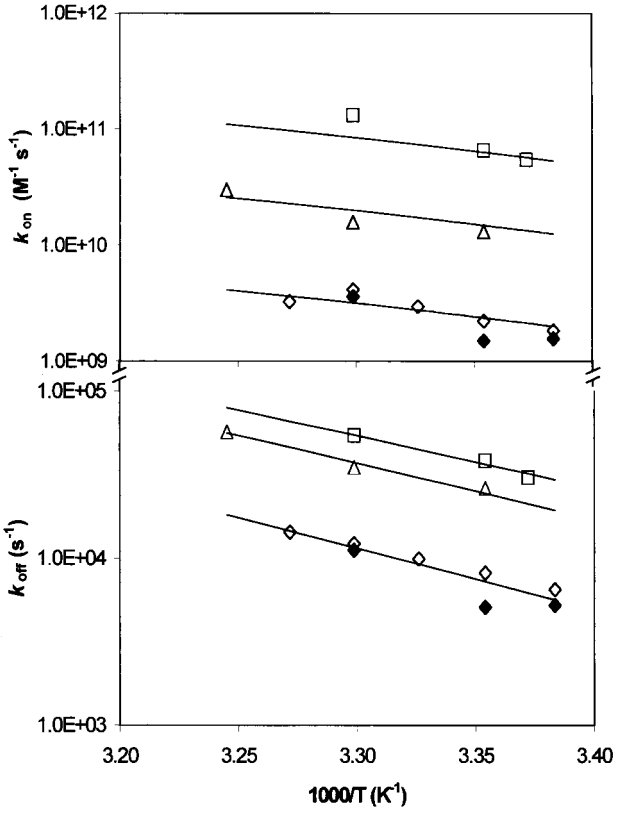

FIGURE 3 k_{on} (*top*) and k_{off} (*bottom*) as a function of T and pH: diamonds (pH 7.0), triangles (pH 4.9), and squares (pH 3.0). The lines represent fits to (*top*) k_{on} using a diffusion controlled reaction model and (*bottom*) k_{off} using a Ferry relation (Eq. 9).

electrostatic charge distribution in the heme pocket, or protein flexibility (Bismuto et al., 1985, 1989). The large values of the distribution width are indicative of a multiplicity of interactions that the fluorophore can undergo with amino acid residues lining the heme pocket in the apoprotein native state or with side chain groups in the "molten globule" (Bismuto et al., 1996). A minor component is present at very short lifetimes with a negative center value. The origin of this component could be explained by dipolar solvent relaxation processes (Lakowicz and Balter, 1982; Lakowicz et al., 1984; Bismuto et a1., 1987), although it may also be due in part to stray light on the detector or other

TABLE 1 Results of fitting the temperature dependence of the off-rate constant to an Arrhenius equation and a Ferry relation

	Arrhenius		Ferry	
pH	Log(A_A) (s^{-1})	E_A (kJ/mol)	Log(A_F) (s^{-1})	E_F (kJ/mol)
7.0	16.1	70	10.1	9.4
5.0	15.5	63	10.1	9.0
3.0	15.1	60	9.9	8.7

There was no significant difference in the quality of the fit.

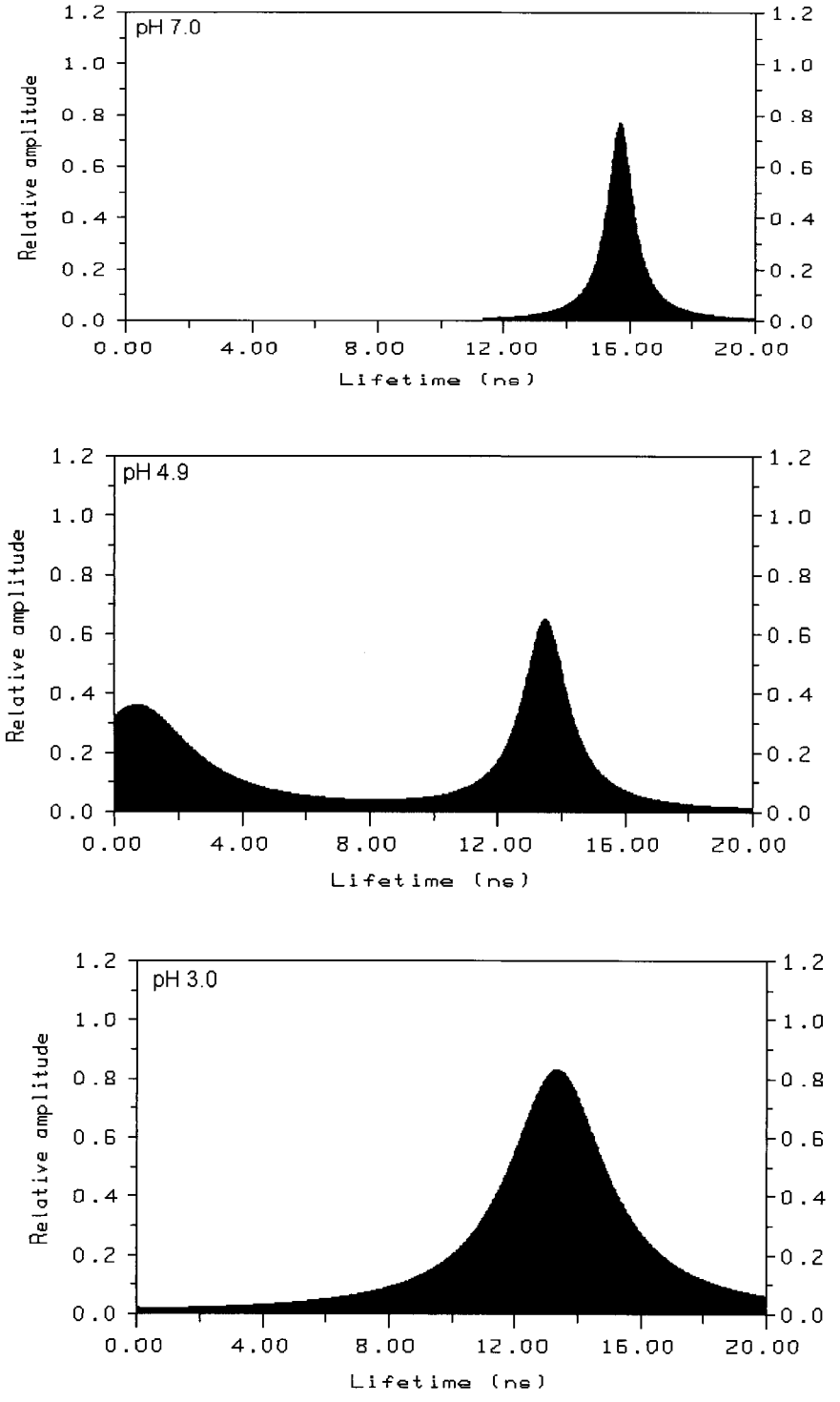

FIGURE 4 pH dependence of the lifetime distribution of the tuna ANS-apomyoglobin complex at 20°C. The excitation wavelength was 295 nm and the emission observed through an optical filter combination of UV34 and UV340. The protein and ANS concentrations were 1 μM.

instrumental artifacts. The minor component increases largely in lifetime as well as in width and population at pH 4.9. This could be related to the appearance of an alternative binding site for the ANS molecule within the large heme pocket region of apomyoglobin. In sperm whale carbonmonoxymyoglobin, H64 and H97 have a pK of 4.5 and 6, respectively (Müller et al., 1997). A protonated histidine destabilizes the heme pocket and increases the amplitude of the conformational fluctuations. The center values for the ANS-apomyoglobin lifetime distribution discussed above differ from those previously reported (Bismuto et al., 1996) probably because in those studies the higher ionic strength and protein concentration could cause a partial self-aggregation of the apomyoglobin ANS complexes.

TABLE 2 Lorentzian bimodal lifetime distribution of tuna ANS-apomyoglobin complex in 10 mM sodium phosphate, 50 mM NaCl. Temperature was 20°C and excitation at 345 nm

	Long-lived component			Short-lived component			
pH	Center	Width	Fraction	Center	Width	Fraction	χ^2
7.0	15.707	1.005	0.770	−0.684	0.050	0.230	0.81
4.9	13.483	1.725	0.642	0.696	4.142	0.358	1.96
3.0	13.339	1.878	0.831	−0.616	0.243	0.169	0.29

The center and full width at half maximum are given in nanoseconds.

DISCUSSION

FCS measures the amplitude and correlation time of fluctuations in fluorescence intensity. Upon binding of ANS to the hydrophobic heme pocket of apomyoglobin, the fluorescence intensity of ANS increases 200-fold. We have used FCS to determine the on and off rate constants of ANS binding to apomyoglobin. The measured ACFs of ANS and tuna apomyoglobin in solution could not be adequately described by diffusion alone, as shown in Fig. 1 and is independent of sample volume and laser power. To extract both k_{on} and k_{off} from the FCS data alone, it is necessary to know the relative intensities of the free ANS and ANS bound to apomyoglobin and to know the concentration of the reagents. From steady-state fluorescence emission experiments, it is known that the fluorescence intensity of ANS increases 200-fold when binding to apomyoglobin with a shift in the peak emission wavelength from 515 to 470 nm. In our two-photon setup, the detection efficiency does not vary strongly in this wavelength region, hence we used a factor of 200 as the difference between the molecular brightnesses of the free and bound ANS molecule. The fractional intensity was determined using Eq. 7. Uncertainties in the concentration arise due to absorption of the protein and ANS to the walls of the sample holder. We minimized this effect by using relatively high concentrations of protein and ANS for the measurements, reducing the fraction of molecules that adhere to the surface of the holder. However, loss of ANS or protein was still observable in some measurements. To correct for this, we let either the ANS concentration or protein concentration vary during fitting.

On and off rate constant determination

The on and off rate constants of ANS to apomyoglobin were determined as a function of pH and temperature as shown in Fig. 3 using Eqs. 4 to 7. The on rate was fitted to a simple diffusion control reaction:

$$k_{on} = 4\pi r_0 (D_L + D_M) f N_A \times 10^{-3}, \quad (8)$$

in which r_0 is the radius of interaction (in centimeters), taken to be 2.2 nm (approximately distance between the centers of apomyoglobin and ANS), D_L and D_M are the respective diffusion coefficients given in cm^2/s, N_A is Avogadro's number, and f is the fraction of interactions that result in binding. The only temperature dependent factor is the viscosity of the buffer that changes the diffusion coefficients. The temperature dependence of the viscosity of water was taken from CRC handbook of Physics and Chemistry (1985), leaving f as the only free parameter in the fit. A fit to Eq. 8 yields values of $f = 0.3$, 1.8, and 8 for pH values of 7, 5, and 3, respectively.

An f value less than one would imply that there is a hindrance to the reaction. The hindrance can either be steric, dynamic, or a combination of both. If the hindrance were only steric, the ANS needs to collide with regions of the apomyoglobin that allow it to migrate to the heme pocket. It may also be, as in the case of the binding of small ligands to myoglobin, that there is no direct access from the solvent to the heme pocket and that the binding of ANS may depend on which conformation the protein is in. If access to the heme pocket is controlled by protein fluctuations and the fluctuations occur on a slower time scale than diffusion of the ligand about the protein, the on rate of ANS binding would be governed by protein fluctuations. If the conformational fluctuations occur quickly so that the probability of finding an open path to the heme pocket during the collision of the ANS molecule with the protein is high, the on rate of ANS will be diffusion limited. As seen in Fig. 3, the temperature dependence of the on rate constant for both pH 7 and pH 5 can be adequately described by the temperature dependence of the diffusion coefficient due to changes in solvent viscosity. If the binding were governed by protein dynamics, we would expect much stronger temperature dependence as observed in the temperature dependence of the off rates. Hence, we conclude that the on rate is diffusion limited and that at pH 7 not every collision results in a binding event. It is not possible to distinguish whether the deviation from unity of the number of collisions that result in binding is due to the probability of finding the right location for binding or finding the protein in the correct conformational substate.

At pH 5, f has a value of 1.8, suggesting that more than one binding site is available in the protein. These results are supported by the lifetime analysis at pH 4.9 where a second binding site is observable with a fluorescent lifetime of $\sim$1 ns. The shorter lifetime of the second binding site implies that the fluorescence from this state is approximately a factor 10 less than when the ANS binds to the heme pocket. However, even with two states available, the number of collisions resulting in a binding event would mean that every event would result in binding of the ANS. This suggests that the protein is either in the open configuration or is much more flexible, making it much easier to bind.

The analysis of the FCS data is based on the assumption that there is one binding site in the protein. At pH 3, the protein is in a partially denatured state with multiple binding sites available that in general will have different fluorescent

intensities. The on rate is too fast to be diffusion limited and is most likely due to protein fluctuations or to the ANS molecule migrating to different binding sites within the partially denatured state. This is consistent with the broad distribution of ANS lifetimes observed in Fig. 4. It is clear that the fundamental assumptions used to derive the model ACF for the bimolecular reaction are no longer valid. Hence, we will limit the remainder of our discussion to the measurements made at pH 7 and pH 4.9.

The temperature dependence of the off rate constant at different pH values is shown in Fig. 3. Dissociation of the ANS molecule from apomyoglobin may be limited by the time scale of thermal fluctuations to overcome the binding enthalpy or may be limited by opening of a pathway to the solvent. The motion involved in opening access between the heme pocket and the solvent requires large protein fluctuations. A similar motion has been measured in sperm whale myoglobin. Carbonmonoxymyoglobin exists in three conformational substates that are observable in the infrared spectra of the CO stretch bands referred to as A_0, A_1, and A_3. Careful analysis of the CO stretch bands reveals the existence of additional substates (Müller et al., 1997), but the additional complexities are not necessary for our discussion. At low pH, band A_0 is dominate and x-ray diffraction shows that the distal histidine (H64) has swung out from the heme pocket into the solvent (Yang and Phillips, 1995). The exchange between A_0 and $A_1 + A_3$ has been measured kinetically from 185 to 280 K (Johnson et al., 1995). Due to the large, complex, and cooperative behavior of the protein fluctuations that occur during the exchange, the temperature dependence of the fluctuation is non-Arrhenius. The data were fit to a Ferry relation (Ferry et al., 1953):

$$k(T) = A_{\mathrm{F}}\exp\left[-\left(\frac{E_{\mathrm{F}}}{kT}\right)^2\right], \qquad (9)$$

in which A_{F} is the preexponential or attempt frequency and E_{F} is the Ferry energy. The fit of the exchange over 11 orders of magnitude in time yielded a preexponential of $A_{\mathrm{F}} = 11.8 \pm 1.4$ and $E_{\mathrm{F}} = 9.3 \pm 0.4$. The macroscopic exchange rate at room temperature in sperm whale myoglobin is $\sim$100,000 s^{-1} at pH 5.7. From the population ratio at room temperature we can calculate $k_{\mathrm{open}} = 5000\ s^{-1}$ and $k_{\mathrm{closed}} = 95{,}000\ s^{-1}$. Due to the large difference in ANS binding rates between species, it is not possible to draw concrete conclusions about whether the opening or the closing of the heme pocket governs the dissociation rate of ANS from tuna apomyoglobin. In principle, the same motion responsible for the swinging of the distal histidine out into the solvent may allow the ligand to escape from the heme pocket. The opposite scenario where the ANS molecule is driven out of the heme pocket when the distal histidine returns into the heme pocket is also conceivable. Without comparing the exchange rate between the open and closed states in tuna myoglobin, it is not possible to determine which scenario is reasonable.

The off rate constant was fit to an Arrhenius and Ferry (Eq. 9) temperature dependences, and the results are given in Table 1. A non-Arrhenius temperature dependence is expected if the dissociation rate is governed by protein fluctuations. There is no difference in the quality of the fit of the two models. However, the preexponentials of $10^{16.1}$ and $10^{15.5}$ at pH 7.0 and pH 5, respectively, are large, suggesting that complex protein motions contribute to the dissociation and that the Ferry relation is more accurate in this case.

Independent of which model is used to describe the temperature dependence, the resulting enthalpy barrier and preexponential or attempt frequency is larger for pH 7 than for pH 5. If protein motions govern the off rate, this would be consistent with a more flexible protein structure at pH 5. With increased flexibility, the energy needed for large global motions decreases, and the resonance or attempt frequency also decreases.

Comparison of horse apomyoglobin to tuna apomyoglobin

From the measured on and off rate constants of ANS binding to tuna apomyoglobin, the reaction rate is significantly higher in tuna apomyoglobin. At pH 7, $k_{\mathrm{on}} = 2200\ \mu M^{-1}\ s^{-1}$ and $k_{\mathrm{off}} = 5900\ s^{-1}$ for tuna apomyoglobin in comparison with $k_{\mathrm{on}} = 640\ \mu M^{-1}\ s^{-1}$ and $k_{\mathrm{off}} = 560\ s^{-1}$ for horse myoglobin (Lamb et al., 2000). If the on rate is diffusion limited in both cases, as suggested by the temperature dependence of the on rate, this implies that the off rate is responsible for the factor 10 difference in the macroscopic reaction rate. Hence, either the ANS binds more strongly in the heme pocket of horse apomyoglobin than it does in tuna apomyoglobin or that the protein fluctuations governing the escape of ANS are slower in horse apomyoglobin. To understand which of these two possibilities is more reasonable (or if both are reasonable) from a protein structure point-of-view, we compared the three-dimensional organization of tuna and horse apomyoglobin after energy minimization of the crystallographic structures without the heme group as described in the methods section. The upper part of Fig. 5 shows the overlapping structures that appear very similar. However, the heme cavity volumes in these structures are quite different, 1626 and 1920 $Å^3$ for tuna and horse apomyoglobin, respectively. Table 3 compares the residues included in a sphere of 6.0 Å of radius surrounding the center of the heme pocket of the two apomyoglobin structures. The presence of a negative charge due to residue D44 in tuna apomyoglobin suggests an unfavorable interaction with the ANS molecule in the heme cavity. Moreover, the protonation of histidine residues in the cavity can explain the alternative ANS binding observed at pH 4.9. The lower part of Fig. 5 shows the electrostatic surface potential for the two apomyoglobin structures calculated as reported in the Materials and Methods section. The surface colors are indicative of electrostatic charges, i.e., red, blue, and white for

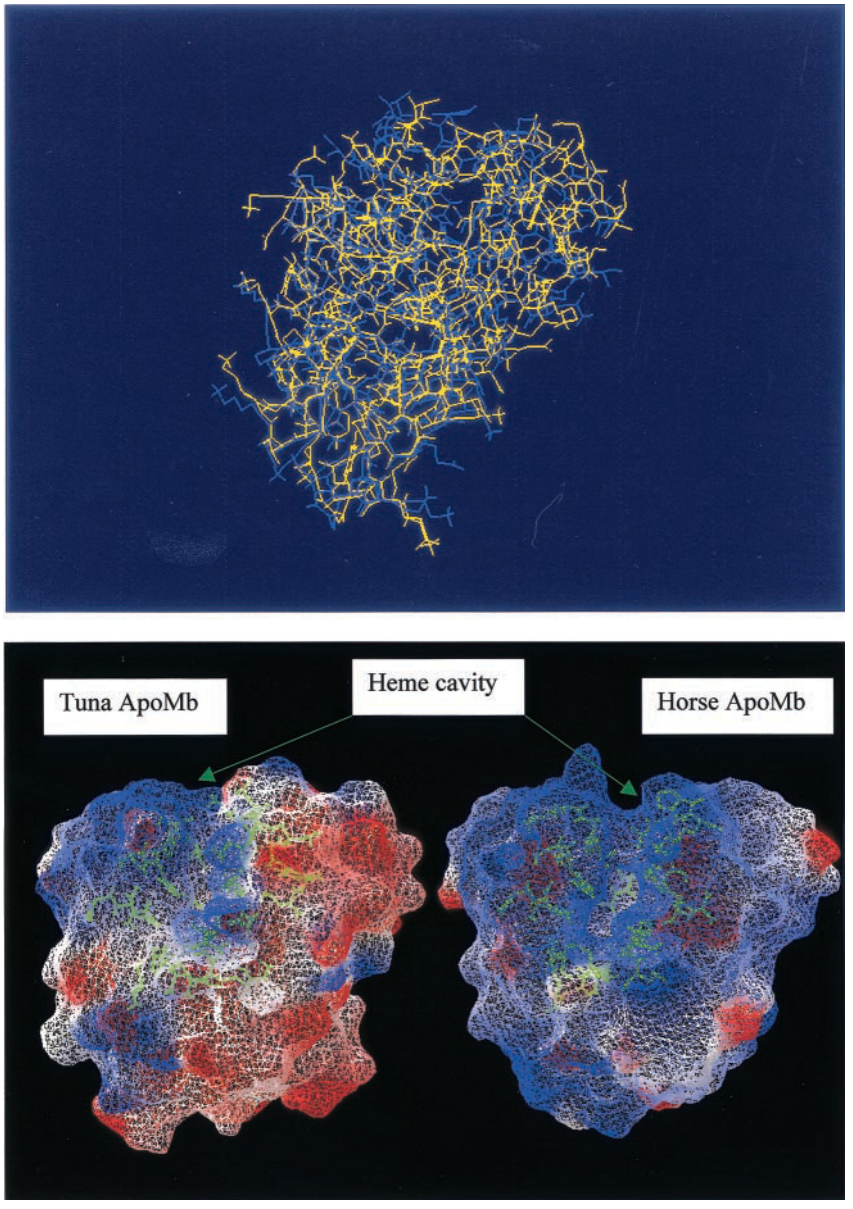

FIGURE 5 (*Top*) Overlapping of tuna (*blue*) and horse (*yellow*) apomyoglobin structures after energy minimization with the GROMOS96 package (Van Gunsteren et al., 1996). The 1MYT and 1YMB pdb files were used to extract starting sets of apomyoglobins coordinates. (*Bottom*) Molecular electrostatic potential surfaces calculated using coulombic potential and only charged residues; the electric potential increases going from red to blue. The solvent and protein dielectric constants were taken as 80 and 4.0, respectively. Molecular surfaces were visualized by Swisse-Pdb-Viewer v3.7b2 (Guex and Peitsch, 1997).

negative, positive, and neutral regions, respectively. A more negative charge density is observed for the smaller heme cavity of tuna apomyoglobin compared with that of horse apomyoglobin.

CONCLUSIONS

Here we affirm the usefulness of FCS in measuring reaction rates. In particular, we have measured the binding of ANS to tuna apomyoglobin as a function of pH and temperature. The on rate appears to be diffusion limited with a temperature dependence of k_{on} that can be described completely through the change in the viscosity of the buffer, whereas k_{off} is influenced, if not totally governed, by protein motions. The differences in the ANS binding rate between tuna and horse apomyoglobins are consistent with frequency domain fluorometry investigations as well as molecular conformational studies by dynamic simulation that shows that the heme removal in tuna apomyoglobin creates a cavity of 15% smaller volume compared with the same cavity in horse myoglobin. Moreover, the protein surface analysis of electrostatic potential evidences a more negative charge density in the heme region of tuna cavity that can hinder the binding of ANS. In conclusion, this paper shows promising new possibilities to explore hydrophobic regions and folding/refolding processes in proteins by ANS fluorescence and FCS. FCS experiments are well suited for denaturation and refolding studies since the measurements can be made in equilibrium and require very dilute concentrations of protein.

TABLE 3 Amino acid residues inside a sphere of 0.6-nm radius surrounding the center of the heme cavity of apomyoglobin

Residue	
Tuna	Horse
L32	**L32**
	F33
T39	**T39**
	L40
L42	K42
F43	**F43**
P44	*D44
K45	**K45**
H64	**H64**
T67	V67
V68	**V68**
L69	**L69**
K71	A71
L72	**L72**
–L75	–I75
P88	**P88**
L89	**L89**
S92	**S92**
H93	**H93**
K96	
H97	**H97**
I99	**I99**
N103	Y103
–F104	–
	L104
I107	**I107**
S108	
	I111
M135	L135
I138	
L142	**L142**

Bold residues are identical in both proteins; similar residues are indicated by a dash; the asterisk underlines the negative charge on residue D44. No marks indicates dissimilar residues.

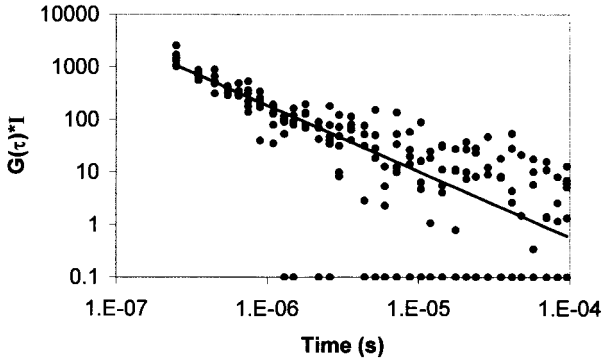

FIGURE 6 The probability density function of afterpulsing of our APD measured at different count rates (*dots*) and a fit to a powerlaw (*solid line*).

APPENDIX

Correction for afterpulsing

Afterpulsing is an artifact observed in both APDs and photomultiplier tubes where an additional pulse is generated by the detector without the detection of a photon. The probability function of afterpulsing varies from detector to detector, but typically has a maximum shortly after a photon has been detected and decays on the 100-ns time scale. Each detected photon has a probability of generating an afterpulse. For our APD, the probability of afterpulsing was 0.2%. Because afterpulsing occurs on the nanosecond timescale, it correlates very strongly. The number of afterpulses is proportional to the average fluorescence intensity. By calculating the autocorrelation function of signal measured from a constant light source, the probability function of afterpulsing can be determined,

$$G_{AP}(\tau) = \frac{\langle I \rangle p_{AP}(\tau)}{\langle I \rangle^2} = \frac{p_{AP}(\tau)}{\langle I \rangle} \qquad (10)$$

in which $p_{AP}(\tau)$ is the probability density function of the arrival of an afterpulse when the detector produced a pulse at $\tau = 0$. The probability density function and afterpulsing for our APD is shown in Fig. 6. What is apparent is that the probability density function has a long tail that can be observable on the 10-μs timescale at low fluorescence intensities.

The most elegant way to remove afterpulsing is to mount a 50/50 beamsplitter in the detection path, add an additional detector, and cross-correlate the signal of the two detectors. However, cross-correlation does not correlate all photons with each other as the autocorrelation function does, hence for the same number of measured photons, the cross-correlation will have a lower signal-to-noise ratio. Another alternative that we found for removing the contribution of afterpulsing to the ACF is to characterize the probability density function (Fig. 6) and subtract the afterpulsing contribution from the ACF. We modeled the tail of the probability density function using a powerlaw (*solid line*, Fig. 6) and subtracted the probability density function divided by the average intensity from the calculated ACF to retrieve the ACF of interest.

We would like to thank Professor Uli Nienhaus and Gaetano Irace for stimulating discussions.

This work was supported by the National Institutes of Health grant RR03155, Italian Research Council (98.01069.CT14), and Italian Ministry of University and Scientific and Technological Research (PRIN2000 "Partly folded states of proteins: analysis by an integrated approach of biochemical and biophysical methods").

REFERENCES

Alcalà, R., E. Gratton, and D. M. Jameson. 1985. A multifrequency phase fluorometer using harmonic content of a mode-locked laser. *Anal. Instrum.* 14:225–250.

Ali, V., K. Prakash, S. Kulkarni, A. Ahmad, K. P. Madhusudan, and V. Bhakuni. 1999. 8-Anilino-1-naphthalene sulfonic acid (ANS) induces folding of acid unfolded cytochrome c to molten globule state as a result of electrostatic interactions. *Biochemistry.* 38:13635–13642.

Aragón, S. R., and R. Pecora. 1976. Fluorescence correlation spectroscopy as a probe of molecular dynamics. *J. Chem. Phys.* 64:1791–1803.

Bedell, J. L., B. S. McCrary, S. P. Edmondson, and J. W. Shriver. 2000. The acid-induced folded state of Sac7d is the native state. *Protein Sci.* 9:1878–1888.

Beechem, J. 1992. Global analysis of biochemical and biophysical data. *Methods Enzymol.* 210:37–54.

Bhattacharyya, A., A. K. Mandal, R. Banerjee, and S. Roy. 2000. Dynamics of compact denatured states of glutaminyl-tRNA synthetase probed by bis-ANS binding kinetics. *Biophys. Chem.* 87:201–212.

Birnbaum G. I., S. V. Evans, M. Przybylska, and D. R. Rose. 1994. 1.70 Angstrom resolution structure of myoglobin from yellowfin tuna: an

example of a myoglobin lacking the D-helix. *Acta. Crystallogr. D. Biol. Crystallogr.* 50:283–289.

Bismuto, E., G. Colonna, F. Savy, and G. Irace. 1985. Myoglobin structure and regulation of solvent accessibility of heme pocket. *Int. J. Pept. Protein Res.* 26:195–207.

Bismuto, E., and G. Irace. 1994. Unfolding pathway of apomyoglobin: simultaneous characterization of acidic conformational states by frequency domain fluorometry. *J. Mol. Biol.* 241:103–109.

Bismuto, E., G. Irace, D. M. Jameson, G. Colonna, and E. Gratton. 1987. Dynamic aspects of the heme binding site in philogenetically distant myoglobins. *Biochim. Biophys. Acta.* 913:324–328.

Bismuto, E., G. Irace, I. Sirangelo, and E. Gratton. 1996. Pressure-induced perturbation of ANS-apomyoglobin complex: frequency domain fluorescence studies on native and acidic compact states. *Protein Sci.* 5:121–126.

Bismuto, E., I. Sirangelo, and G. Irace. 1989. Conformational substates of myoglobin detected by extrinsic dynamic fluorescence studies. *Biochemistry.* 28:7542–7545.

Bonnet, G., O. Krichevsky, and A. Libchaber. 1998. Kinetics of conformational fluctuations in DNA hairpin-loops. *Proc. Natl. Acad. Sci. U.S.A.* 95:8602–8606.

Broos, J., G. B. Strambini, M. Gonelli, G. S. Wolters, E. P. P. Vos, and G. T. Robillard. 2001. Studying membrane transport protein dynamics with tryptophan phosphorescence specroscopy. *Biophys. J.* 80(Part 2): 1050.

Cioni, P., and G. B. Strambini. 1998. Acrylamide quenching of protein phosphorescence as a monitor of structural fluctuations in the globular fold. *J. Am. Chem. Soc.* 120:11749–11757.

Clarke, D., A. Doig, B. Stapley, and G. Jones. 1999. The α-elix folds on the millisecond time scale. *Proc. Natl. Acad. Sci. U.S.A.* 96:7232–7237.

Cooper, A., and J. Hoube. 1988. Enzyme catalysis: the view from physical chemistry: the enzyme catalysis process: energetics, mechanism, and dynamics. *NATO Adv. Sci. Inst. Ser.* 178:3–21.

Demarest, S. J., J. C. Horng, and D. P. Raleigh. 2001. A protein dissection study demonstrates that two specific hydrophobic clusters play a key role in stabilizing the core structure of the molten globule state of human alpha-lactalbumin. *Proteins.* 42:237–242.

Ehrenberg, M., and R. Rigler. 1974. Rotational: Brownian motion and fluorescence intensity fluctuations. *Chem. Phys.* 4:390–401.

Elson, E. L., and D. Madge. 1974. Fluorescence correlation spectroscopy: I. Conceptual basis and theory. *Biopolymers.* 13:1–27.

Evans, S., and G. Brayer. 1990. High-resolution study of three-dimensional structure of horse heart metmyoglobin. *J. Mol. Biol.* 213:885–897.

Farazi, T., J. Manchester, and J. Gordon. 2000. Transient kinetic analysis of *Saccharomices cerevisiae* myristoylCoA: protein *N*-myristoiltransferase reveals that a step after chemical transformation is rate limiting. *Biochemistry.* 39:15807–15816.

Ferry, J. D., L. D. Grandine, and E. R. Fitzgerald. 1953. The relaxation distribution function of polyisobuylene in the transition from rubber-like to glass-like behavior. *J. Appl. Phys.* 24:911–916.

Gratton, E., and M. Limkeman. 1983. A continuously variable frequency cross-correlation phase fluorometer with picosecond resolution. *Biophys. J.* 44:315–324.

Guex, N., and M. C. Peitsch. 1997. SWISS-MODEL and the Swisse-Pdb Viewer: an environment for comparative protein modeling. *Electrophoresis.* 18:2714–2723.

Haupts, U., S. Maiti, P. Schwille, and W. W. Webb. 1998. Dynamics of fluorescence fluctuations in green fluorescent protein observed by fluorescence correlation spectroscopy. *Proc. Natl. Acad. Sci. U.S.A.* 95: 13573–13578.

Hiromi, K. 1979. Kinetics of fast enzyme reactions: theory and practice. Wiley and Sons, New York.

Holtzer, M., G. Bretthorst, A. d'Avignon, R. Angeletti, L. Mints, and A. Holtzer. 2001. Temperature dependence of the folding and unfolding kinetics of the GCN4 leucine zipper via $^{13}C^{\alpha}$-NMR. *Biophys. J.* 80: 939–951.

Hughson, F., P. Wright, and R. Baldwin. 1990. Structural characterization of partly folded apomyoglobin intermediate. *Science.* 249:1544–1548.

Jaenicke, R., and H. Lilie. 2000. Folding and association of oligomeric and multimeric proteins. *Adv. Protein Chem.* 53:329–401.

Johnson, J. B., D. C. Lamb, H. Frauenfelder, J. D. Müller, B. McMahon, G. U. Nienhaus, and R. D. Young. 1995. Ligand binding to heme proteins: VI. Interconversion of taxonomic substates in carbonmonoxymyoglobin. *Biophys. J.* 71:1563–1573.

Kask, P., P. Piksarv, M. Pooga, Ü. Mets, and E. Lippmaa. 1989. Separation of the rotational contribution in fluorescence correlation experiments. *Biophys. J.* 55:213–220.

Khan, F., R. H. Khan, and S. Muzammil. 2000. Alcohol-induced versus anion-induced states of alpha-chymotrypsinogen A at low pH. *Biochim. Biophys. Acta.* 1481:229–236.

Kundu, B., and P. Guptasarma. 1999. Hydrophobic dye inhibits aggregation of molten carbonic anhydrase during thermal unfolding and refolding. *Proteins.* 37:321–324.

Lakowicz, J. R., and A. Balter. 1982. Analysis of excited-state processes by phase-modulation fluorescence spectroscopy. *Biophys. Chem.* 16: 99–115.

Lakowicz, J. R., E. Gratton, H. Cherek, B. P. Maliwal, and G. Laczko. 1984. Determination of time-resolved fluorescence emission spectra and anisotropies of a fluorophore-protein complex using frequency-domain phase-modulation fluorometry. *J. Biol. Chem.* 259:10967–10972.

Lamb, D., A. Schenk, C. Röcker, C. Scalfi-Happ, and G. U. Nienhaus. 2000. Sensitivity enhancement in fluorescence correlation spectroscopy of multiple species using time-gated detection. *Biophys. J.* 79: 1129–1138.

Li, Y., and G. Jing. 2000. Double point mutant F34W/W140F of staphylococcal nuclease is in a molten globule state but highly competent to fold into a functional conformation. *J. Biochem. (Tokyo).* 128:739–744.

Lide, D. R. 1985. Handbook of Chemistry and Physics. CRC Press, N.Y.

Magde, D. 1976. Chemical kinetics and fluorescence correlation spectroscopy. *Quart. Rev. Biophys.* 9:35–47.

Magde, D., E. L. Elson, and W. W. Webb. 1972. Thermodynamic fluctuations in a reacting system: measurement by fluorescence correlation spectroscopy. *Phys. Rev. Lett.* 29:705–708.

Magde, D., E. L. Elson, and W. W. Webb. 1974. Fluorescence correlation spectroscopy: II. An experimental realization. *Biopolymers.* 13:29–61.

Müller, J. D., B. H. McMahon, Y. E. T. Chien, S. G. Sligar, and G. N. Nienahus. 1997. Connection between the taxonomic substates and protonation of histidines 64 and 97 in carbonmonoxy myoglobin. *Biophys. J.* 77:1036–1051.

Muzammil, S., Y. Kumar, and S. Tayyab. 1999. Molten globule-like state of human serum albumin at low pH. *Eur. J. Biochem.* 266:26–32.

Rauer, B., E. Neumann, J. Widengren, and R. Rigler. 1996. Fluorescence correlation spectrometry of the interaction kinetics of tetramethylrhodamin α-bungarotoxin with *Torpedo californica* acetylcholine receptor. *Biophys. Chem.* 58:3–12.

Rigler, R., U. Mets, J. Widengren, and P. Kask. 1993. Fluorescence correlation spectroscopy with high count rate and low-background: analysis of translational diffusion. *Eur. Biophys. J.* 22:169–175.

Safar, J., P. P. Roller, D. C. Gajdusek, and C. J. Gibbs Jr. 1994. Scrapie amyloid (prion) protein has the conformational characteristics of an aggregated molten globule folding intermediate. *Biochemistry.* 33: 8375–8383.

Stryer, K. 1965. The interaction of a naphthalene dye with apomyoglobin and apohemoglobin: a fluorescent probe of non-polar binding sites. *J. Mol. Biol.* 13:482–495.

Teale, F. W. J. 1959. Cleavage of the heme-protein link by acid methylethylketone. *Biochim. Biophys. Acta.* 35:543.

Thompson, N. L. 1991. Fluorescence correlation spectroscopy. *In* Topics in Fluorescence Spectrocopy Techniques, Vol. 1. J. R. Lakowicz, editor. Plenum Press, New York. 337–378.

Van Gunsteren, W. F., S. R. Billeter, A. Eising, P. Hünenberger, P. Krüger, A. Mark, W. Scott, and I. Tironi. 1996. *In* Biomolecular Simulation: the GROMOS96 Manual and User Guide, Vdf Hochschulverlang ETHZ, Zürich.

Weber, G., and L. R. Young. 1964. Fragmentation of bovine serum albumin by pepsin. *J. Biol. Chem.* 239:1415–1421.

Wetlaufer, D. B. 1962. Ultraviolet spectra of proteins and amino acids. *Adv. Protein Chem.* 17:303–390.

Widengren, J., Ü. Mets, and R. Rigler. 1995. Fluorescence correlation spectroscopy of triplet states in solution: a theoretical and experimental study. *J. Phys. Chem.* 99:13368–13379.

Widengren, J., R. Rigler, and Ü. Mets. 1994. Triplet-state monitoring by fluorescence correlation spectroscopy. *J. Fluoresc.* 4:255–258.

Yang, F., and G. N. Phillips Jr. 1995. Structures of CO-, deoxy-, and met-myoglobin at various pH values. *J. Mol. Biol.* 256:762–774.

Zhou, B., K. Tian, and G. Jing. 2000. An in vitro peptide folding model suggests the presence of the molten globule state during nascent peptide folding. *Protein Eng.* 13:35–39.